Electronic Supplementary Material (ESI) for Dalton Transactions
This journal is © The Royal Society of Chemistry 2012

Comparative Study of Different Methods for the Preparation of Tetraamidato- and Tetracarboxylatodiruthenium Compounds. Structural and Magnetic Characterization

Patricia Delgado,[a] Rodrigo González-Prieto,[a] Reyes Jiménez-Aparicio,[a,*] Josefina Perles,[a] José L. Priego,[a,*] and Rosario M. Torres.[b]

[a]*Departamento de Química Inorgánica, Facultad de Ciencias Químicas, Universidad Complutense de Madrid, Ciudad Universitaria, E-28040 Madrid, Spain. E-mail: reyesja@quim.ucm.es; bermejo@quim.ucm.es*

[b]*Centro de Asistencia a la Investigación de Rayos X. Facultad de Ciencias Químicas. Universidad Complutense de Madrid. Ciudad Universitaria, 28040 Madrid, Spain.*

Electronic Supplementary Information:

Representation of the structure of complexes **3**, **5** and **6**

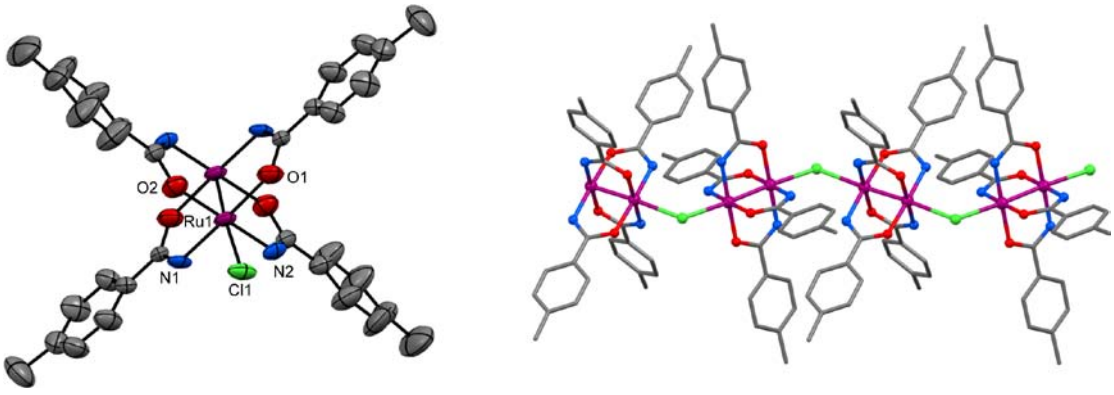

Figure S1. Left: thermal-ellipsoid representation of the structure of $[Ru_2Cl(\mu\text{-}NHOCC_6H_4\text{-}p\text{-}Me)_4]$ (**3**), (50% probability ellipsoids). Right: drawing of a zig-zag $[Ru_2Cl(\mu\text{-}NHOCC_6H_4\text{-}p\text{-}Me)_4]_n$ chain. Hydrogen atoms are omitted for clarity.

This journal is © The Royal Society of Chemistry 2012

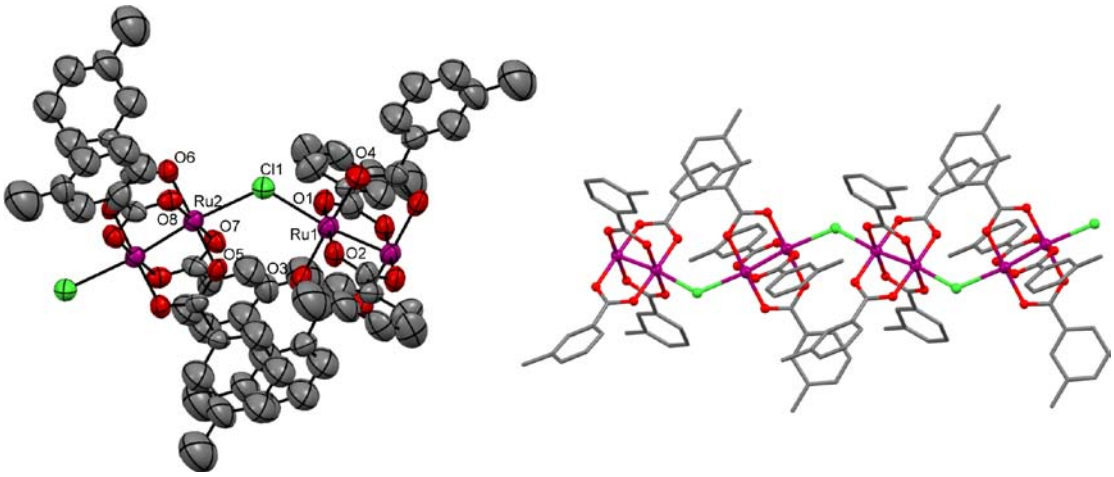

Figure S2 Left: thermal-ellipsoid representation of the structure of $[Ru_2Cl(\mu\text{-}O_2CC_6H_4\text{-}m\text{-}Me)_4]$ (**5**), (50% probability ellipsoids). Right: drawing of a zig-zag $[Ru_2Cl(\mu\text{-}O_2CC_6H_4\text{-}m\text{-}Me)_4]_\infty$ chain. Hydrogen atoms are omitted for clarity.

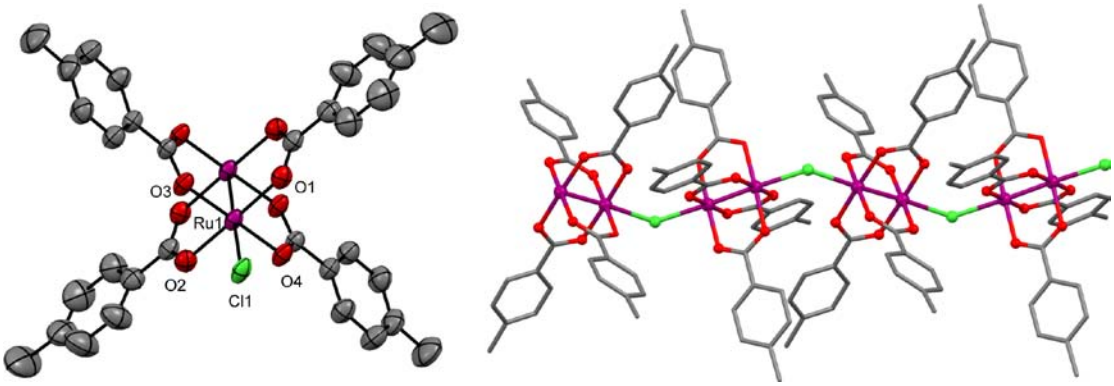

Figure S3. Left: thermal-ellipsoid representation of the structure of $[Ru_2Cl(\mu\text{-}O_2CC_6H_4\text{-}p\text{-}Me)_4]$ (**6**), (50% probability ellipsoids). Right: drawing of a zig-zag $[Ru_2Cl(\mu\text{-}O_2CC_6H_4\text{-}p\text{-}Me)_4]_\infty$ chain. Hydrogen atoms are omitted for clarity.

This journal is © The Royal Society of Chemistry 2012

Experimental and calculated curves for complexes **1** and **3-6**

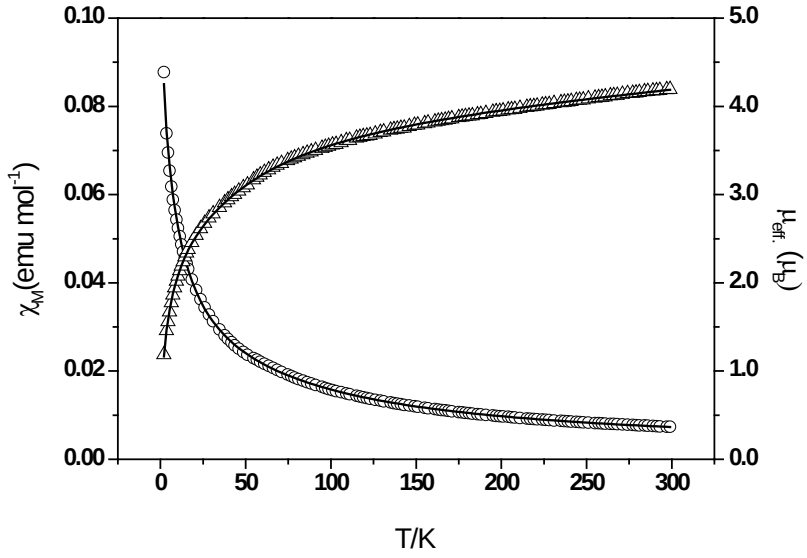

Figure S4. Temperature dependence of the molar susceptibility χ_M (circles) and $\mu_{eff.}$ (triangles) for complex **3**; solid lines are the product of a least-squares fit to the model indicated in the text.

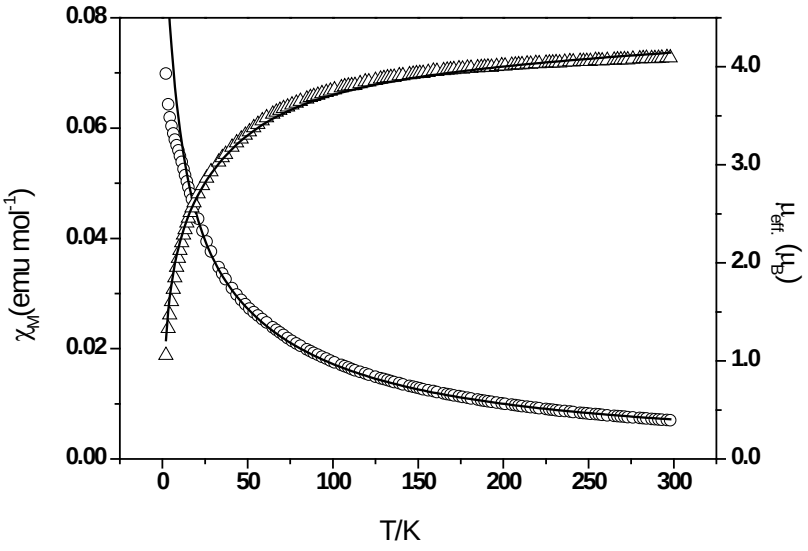

Figure S5. Temperature dependence of the molar susceptibility χ_M (circles) and $\mu_{eff.}$ (triangles) for complex **4**; solid lines are the product of a least-squares fit to the model indicated in the text.

This journal is © The Royal Society of Chemistry 2012

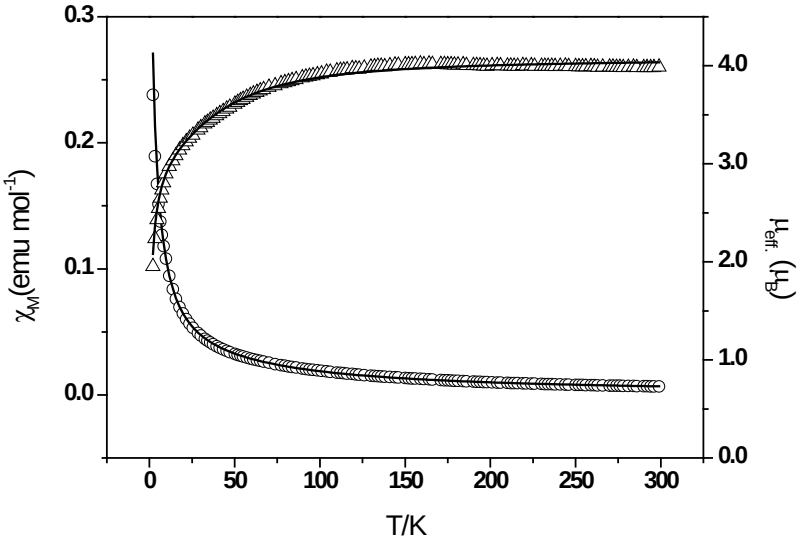

Figure S6. Temperature dependence of the molar susceptibility χ_M (circles) and $\mu_{eff.}$ (triangles) for complex **5**; solid lines are the product of a least-squares fit to the model indicated in the text.

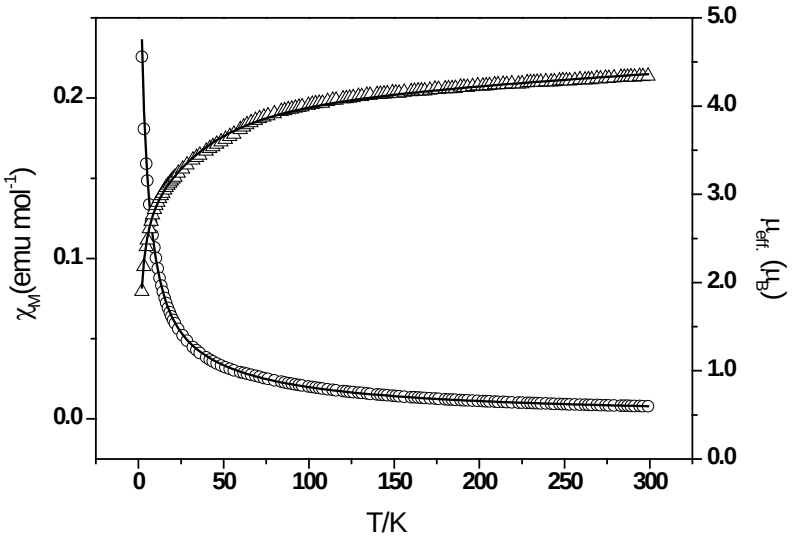

Figure S7. Temperature dependence of the molar susceptibility χ_M (circles) and $\mu_{eff.}$ (triangles) for complex **6**; solid lines are the product of a least-squares fit to the model indicated in the text.

This journal is © The Royal Society of Chemistry 2012

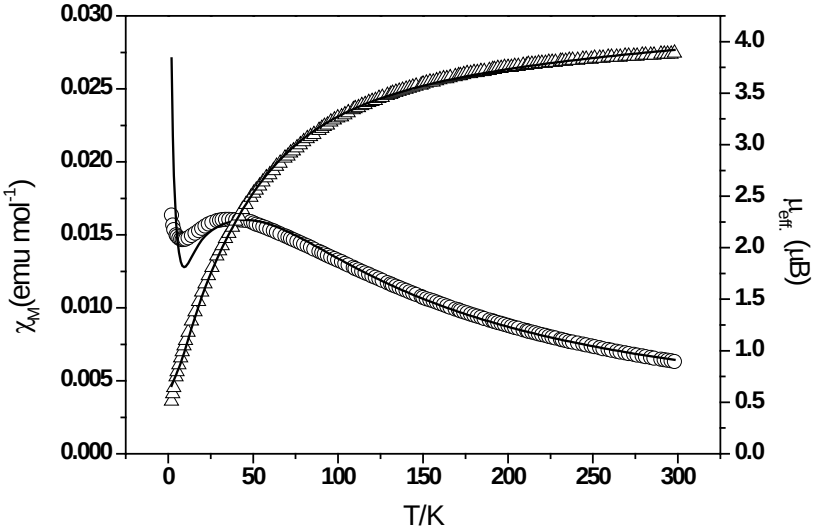

Figure S8. Temperature dependence of the molar susceptibility χ_M (circles) and $\mu_{eff.}$ (triangles) for complex **1**. Fit were made considering a mononuclear paramagnetic impurity with S=1/2; solid lines are the product of a least-squares fit to the model indicated in the text.

This journal is © The Royal Society of Chemistry 2012

Experimental and calculated diffractogram of complexes **1** - **6**

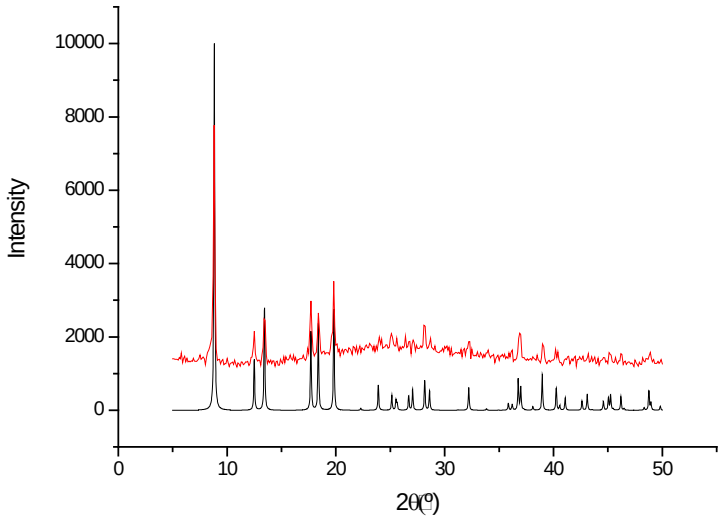

Figure S9. Red: Experimental data of X-ray powder diffractometry of compound **1**. Black: Diffractogram simulated from single crystal X-ray determination

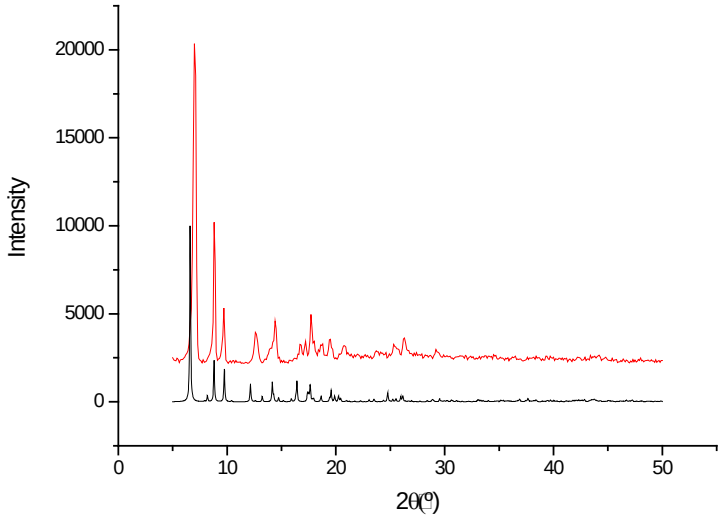

Figure S10. Red: Experimental data of X-ray powder diffractometry of compound **2**. Black: Diffractogram simulated from single crystal X-ray determination

This journal is © The Royal Society of Chemistry 2012

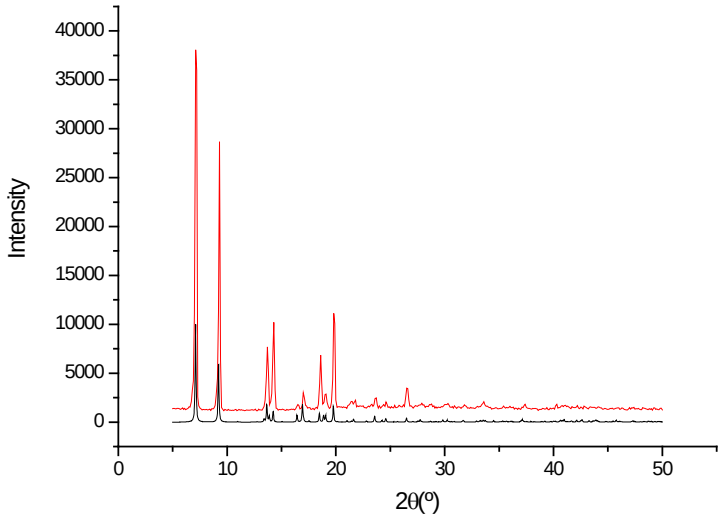

Figure S11. Red: Experimental data of X-ray powder diffractometry of compound **3**. Black: Diffractogram simulated from single crystal X-ray determination

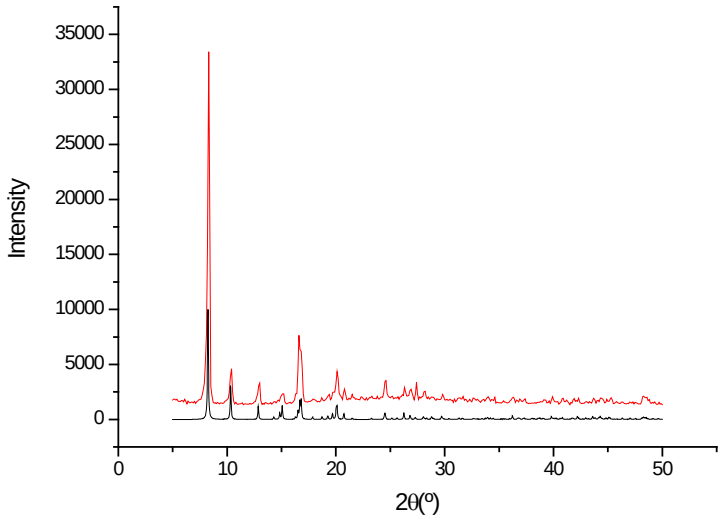

Figure S12. Red: Experimental data of X-ray powder diffractometry of compound **4**. Black: Diffractogram simulated from single crystal X-ray determination

This journal is © The Royal Society of Chemistry 2012

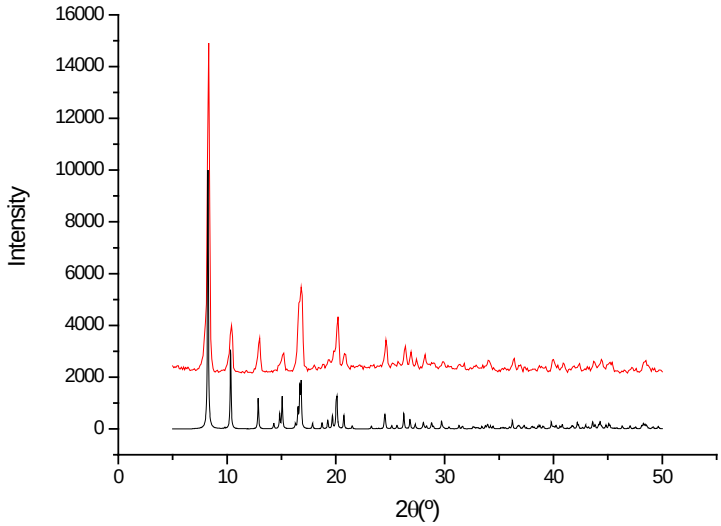

Figure S13. Red: Experimental data of X-ray powder diffractometry of compound **5**. Black: Diffractogram simulated from single crystal X-ray determination

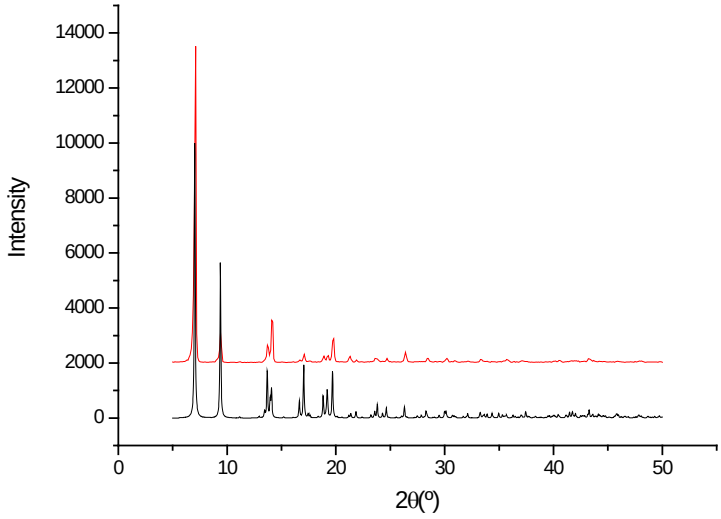

Figure S14. Red: Experimental data of X-ray powder diffractometry of compound **6**. Black: Diffractogram simulated from single crystal X-ray determination